PHILOSOPHICAL TRANSACTIONS A

royalsocietypublishing.org/journal/rsta

Research

**Cite this article:** Zubarev AY. 2019 Effect of internal chain-like structures on magnetic hyperthermia in non-liquid media. *Phil. Trans. R. Soc. A* **377**: 20180213.
http://dx.doi.org/10.1098/rsta.2018.0213

Accepted: 25 October 2018

One contribution of 17 to a theme issue 'Heterogeneous materials: metastable and non-ergodic internal structures'.

**Subject Areas:**
thermodynamics, medical physics

**Keywords:**
magnetic hyperthermia, interparticle interaction, morphology of particle spatial disposition

**Author for correspondence:**
Andrey Yu. Zubarev
e-mail: a.j.zubarev@urfu.ru

THE ROYAL SOCIETY PUBLISHING

# Effect of internal chain-like structures on magnetic hyperthermia in non-liquid media

Andrey Yu. Zubarev[1,2]

[1]Laboratory of Multi-Scale Mathematical Modeling, Department of Theoretical and Mathematical Physics, Ural Federal University, Lenin Avenue 51, Ekaterinburg 620083, Russian Federation
[2]M.N. Mikheev Institute of Metal Physics of the Ural Branch of the Russian Academy of Sciences, Ekaterinburg, Russian Federation

AYuZ, 0000-0001-5826-9852

This paper deals with a theoretical study of the effect of chain-like aggregates on magnetic hyperthermia in systems of single-domain ferromagnetic particles immobilized in a non-magnetic medium. We assume that the particles form linear chain-like aggregates and the characteristic time of the Néel remagnetization is much longer than the time of medium heating (time of process observation). This is applicable to magnetite particles when the particle diameter exceeds 20–25 nm. Our results show that the appearance of the chains significantly decreases the intensity of heat production.

This article is part of the theme issue 'Heterogeneous materials: metastable and non-ergodic internal structures'.

## 1. Introduction

Magnetic hyperthermia is a very promising method for curing cancer diseases [1,2]. The main idea behind this approach is in embedding magnetic nanoparticles in the tumour area and heating the particles (and the tumour cells) by an alternating magnetic field. Numerous investigations show that in the temperature range 42–50°C the tumour cells die, whereas the healthy cells survive [3–7]. This is the key point of the therapeutic effect.

There are two main physical mechanisms of heat production. The first one is induced by the rotation of the particles, under the action of the field, in the carrier

medium and energy dissipation because of the effects of the medium viscosity. The second one relies on the dissipation effects of the internal remagnetization of particles. The viscous (very often called Brownian) mechanism is typical for relatively large ferromagnetic particles suspended in a liquid medium (see details in [8,9]). The second, internal, mechanism is typical for small particles in liquids or for any particles immobilized in a rigid medium.

Being embedded in a biological environment, magnetic nanoparticles, as a rule, are tightly bound to the surrounding tissues [10,11]. Thus, the case of immobilized particles and the heat production due to their internal remagnetization is the most interesting from the viewpoint of the biomedical application of magnetic hyperthermia.

The majority of known theoretical studies of this phenomenon deal with the simplest systems of non-interacting particles, remagnetized according to the Néel mechanism (see, for example, [8,12,13]). Recently, the effect of the magnetic interparticle interaction on the heat production due to this mechanism of remagnetization has been studied [14]. It was shown that the heat production is most efficient when the particle axis of easy magnetization is parallel to the direction of the oscillating field; magnetic interaction between the particles enhances the heat production.

Let us discuss and summarize the main features of Néel remagnetization. The energy of a single uniaxial ferromagnetic particle can be represented [15] as follows:

$$U = -\mu_0 M_s v_p (\boldsymbol{m} \cdot \boldsymbol{H}) + U_a, \quad U_a = -K v_p (\boldsymbol{m} \cdot \boldsymbol{n})^2.$$

Here, $\mu_0$ is the vacuum magnetic permeability; $M_s$ is the saturated magnetization of the particle material; $v_p$ is the particle volume; $\boldsymbol{m}$ is the unit vector aligned along the magnetic moment of the particle; $\boldsymbol{H}$ is the field acting on the particle; $K$ is the parameter of the particle magnetic anisotropy; and $\boldsymbol{n}$ is the unit vector directed along the particle axis of easy magnetization. The second term on the right of this expression is the energy of the particle interaction with the field $\boldsymbol{H}$; $U_a$ is the energy of the particle internal magnetic anisotropy.

The energy $U_a$ has two minima, corresponding to the parallel and antiparallel orientations of the vectors $\boldsymbol{n}$ and $\boldsymbol{m}$. At low fields, when the inequality $\mu_0 M_s H < K$ holds, the transition between these potential wells is possible only because of the thermal fluctuations of the vector $\boldsymbol{m}$; the characteristic time $\tau_N$ of this transition (Néel time of the particle moment relaxation) is [16]

$$\tau_N = \tau_0 \exp\left(\frac{K v_p}{k T^o}\right), \quad \tau_0 \sim 10^{-9}\,\mathrm{s}.$$

Here, $kT^o$ is the absolute temperature in energetic units.

Typically, *magnetite* particles are used in medical applications of magnetic hyperthermia. First, because they are not toxic; secondly, they are relatively cheap; and, next, they have magnetic moments sufficient to provide a link with the magnetic fields easily achievable in the laboratory and clinical conditions. It was concluded in [17–19] that particles with a diameter in the range 25–30 nm are most efficient for these applications.

By using $K \approx 14\,\mathrm{kJ\,m^{-3}}$ [9] for the magnetite particles, one obtains $\tau_N \sim 2.7 \times 10^3 - 3 \times 10^{12}\,\mathrm{s}$ for particles with a diameter in the range 25–30 nm. These values of $\tau_N$ exceed the typical time of the real hyperthermia process, which usually is about half an hour. Thus, the estimates of the thermal effect, based on the concept of the Néel remagnetization, cannot be used when the heating is provided by particles of this size.

In this work, we consider the heat production in a system of ferromagnetic particles whose time of the Néel remagnetization is much more than the real time of the process of tissue heating. Simple estimates show that the energy of magnetic interaction between magnetite particles with a diameter in the range 20–30 nm is significantly more than the thermal energy of the human body. Therefore, after particle injection, under the action of magnetic forces, they can form various heterogeneous structures, detected in ferrofluids—linear chains, branched and dense clusters, etc. It should be noted that the question of the effect of the magnetic interaction between the particles on the produced thermal effect is disputed in the literature. An increase of energy adsorption has been detected in [20,21]; a decrease in [22,23]; and a non-monotonic dependence of the heat production on the interaction in [24]. It appears that this effect is very sensitive to the morphology

of particle spatial disposition. In this work, we study theoretically the effect of linear chains on the hyperthermia in a system of nanoparticles.

## 2. Magnetic hyperthermia

The intensity $W$ of heat production (the heat production per unit time in unit volume of the system) can be determined on the basis of the general relation of thermodynamics of magnetizable media [15] (see also [8]):

$$W = -\frac{\mu_0}{T}\Phi\int_0^T M_z(t)\frac{\mathrm{d}H}{\mathrm{d}t}\mathrm{d}t. \tag{2.1}$$

Here, $\Phi$ is the volume concentration of the particles, $T$ is the time, much longer than the period of the alternating field; and $M_z$ is the magnetization of an arbitrary particle in the direction of the field $\boldsymbol{H}$ in the sample. We will use a coordinate system with the axis $Oz$ in the $\boldsymbol{H}$ direction and suppose that the field alternates as $\boldsymbol{H} = \boldsymbol{H}_0\cos\Omega t$, where $\boldsymbol{H}_0$ and $\Omega$ are the amplitude and angular frequency of the field, respectively.

It will be convenient to use the following dimensionless variables:

$$\tau = \frac{t}{t_0}, \quad \omega = \Omega t_0, \quad \boldsymbol{h}_0 = \frac{\boldsymbol{H}_0}{M_\mathrm{s}}, \tag{2.2}$$

where $M_\mathrm{s}$ is the saturated magnetization of the particle and $t_0 = 1/\mu_0\gamma M_\mathrm{s} \approx 9\times10^{-10}$ s; $\beta = 2K/\mu_0 M_\mathrm{s}^2 \approx 0.11$. The numerical values of $t_0$ and $\beta$ are estimated for the magnetite particles; $\gamma$ is the gyroscopic ratio.

By using the dimensionless variables (2.2) and $\boldsymbol{H} = \boldsymbol{H}_0\cos\Omega t$, one can represent (2.1) as follows:

$$\left.\begin{aligned} W &= \mu_0\Phi\frac{M_\mathrm{s}^2}{t_0}w, \\ w &= -\frac{1}{\Theta}\int_0^\Theta m_z\frac{\mathrm{d}h}{\mathrm{d}\tau}\mathrm{d}\tau = \frac{\omega h_0}{\Theta}\int_0^\Theta m_z\sin\omega\tau\,\mathrm{d}\tau, \\ m_z &= \frac{M_z}{M_\mathrm{s}}, \quad \Theta = \frac{T}{t_0}. \end{aligned}\right\} \tag{2.3}$$

Here, $w$ is the dimensionless intensity of heat release per particle.

Thus, to determine the intensity $W$ of the heat production, one needs to find the time-dependent component $m_z(t)$ of the unit vector $\boldsymbol{m}$ of a particle and to calculate the integral (2.3).

## 3. Single particle

Let us start solving this problem with the approximation of non-interacting particles.

Estimates show that the Zeeman energy $\mu_0 M_\mathrm{s} v_\mathrm{p} H$ of a magnetite particle with diameter $d \sim 20$ nm exceeds the thermal energy $kT^\mathrm{o}$ if the field $H$ is more than 2 kA m$^{-1}$. The typical strength of the magnetic fields used in medical applications lies in the range 2–15 kA m$^{-1}$ (see, for example, [17,23]). Thus, for the particles with diameter $d \geq 20$ nm, in the first approximation, one can neglect the thermal fluctuations of the direction of the particle magnetic moment.

Neglecting here and below thermal fluctuations of the unit vector $\boldsymbol{m}$, we will describe its dynamics by using the classical Landau–Lifshitz equation [25] (see also [26,27]). In the dimensionless variables (2.2), this equation reads as follows:

$$\left.\begin{aligned} \frac{\mathrm{d}\boldsymbol{m}}{\mathrm{d}\tau} &= -[\boldsymbol{m}\times\boldsymbol{h}^\mathrm{eff}] - \lambda[\boldsymbol{m}\times[\boldsymbol{m}\times\boldsymbol{h}^\mathrm{eff}]], \\ \boldsymbol{h}^\mathrm{eff} &= \boldsymbol{h}_0\cos\omega\tau + \beta\boldsymbol{n}(\boldsymbol{m}\cdot\boldsymbol{n}). \end{aligned}\right\} \tag{3.1}$$

Here, $\boldsymbol{h}^\mathrm{eff}$ is the effective field acting on the particle; the first term $\boldsymbol{h}_0\cos\omega\tau$ is the dimensionless alternating field in the sample; the term $\beta\boldsymbol{n}(\boldsymbol{m}\cdot\boldsymbol{n})$ is a dimensionless field of the particle magnetic anisotropy; $\lambda$ is a dimensionless dissipation parameter.

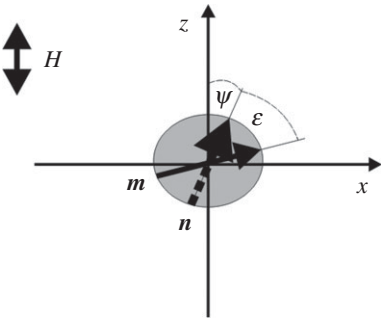


**Figure 1.** Sketch of the particle placed in the linearly polarized field *H*.

We will use the Cartesian coordinate system with the axis $Oz$ aligned along the direction of the field $\boldsymbol{H}$, and axis $Ox$ aligned in the plane formed by the vectors $\boldsymbol{H}$ and $\boldsymbol{n}$ (see figure 1).

It will be convenient also to introduce the spherical coordinate system for the vector $\boldsymbol{m}$ as follows:

$$m_x = \sin\theta\sin\varphi, \quad m_y = \sin\theta\sin\varphi, \quad m_z = \cos\theta. \tag{3.2}$$

Here, $\theta$ and $\varphi$ are the polar and azimuthal angles, respectively.

In this spherical coordinate system, the vector equation (3.1) can be written as follows:

$$\left.\begin{aligned} \frac{\mathrm{d}\theta}{\mathrm{d}\tau} &= -h_x^{\mathrm{eff}}\sin\varphi + \lambda(h_x^{\mathrm{eff}}\cos\theta\cos\varphi - h_z^{\mathrm{eff}}\sin\theta),\\ \sin\varphi\frac{\mathrm{d}\varphi}{\mathrm{d}\tau} &= -(h_x^{\mathrm{eff}}\cos\theta\cos\varphi - h_z^{\mathrm{eff}}\sin\theta) - \lambda h_x^{\mathrm{eff}}\sin\varphi,\\ h_z^{\mathrm{eff}} &= h_0\cos\omega\tau + \beta n_z(n_z\cos\theta + n_x\sin\theta\cos\varphi),\\ h_x^{\mathrm{eff}} &= \beta n_x(n_z\cos\theta + n_x\sin\theta\cos\varphi). \end{aligned}\right\} \tag{3.3}$$

Equations (3.3) present a system of nonlinear differential equations with respect to the angles $\theta$ and $\varphi$. In the general case, this system can be solved only numerically.

To get some analytical results, we will restrict ourselves to the case of relatively weak fields, when the inequality $\mu_0 M_s H_0 < K$ holds. By using here the values of $K$ and $M_s$ for the magnetite particles, we come to the restriction for the field amplitude $H_0 < 20\,\mathrm{kA\,m^{-1}}$. Note that the typical strengths of the fields used in medical applications of magnetic hyperthermia are in the region of $15\,\mathrm{kA\,m^{-1}}$, i.e. the inequality $H_0 < 20\,\mathrm{kA\,m^{-1}}$ is satisfied.

By using the dimensionless variables (2.2), the inequality $\mu_0 M_s H_0 < K$ can be rewritten as $h_0 < \beta$. Let us suppose that the strong inequality $h_0 \ll \beta$ holds. In the absence of the applied magnetic field ($h_0 = 0$), the vector $\boldsymbol{m}$ must be aligned along the vector $\boldsymbol{n}$ of the particle axis of easy magnetization. This means that without the field the equality $\theta = \psi$ must hold. Here, $\theta$ is the angle between the vectors $\boldsymbol{n}$ and $\boldsymbol{H}$; $n_x = \sin\psi$, $n_z = \cos\psi$ (see figure 1).

Because of the strong inequality $h_0 \ll \beta$, the field-induced deviation of the vector $\boldsymbol{m}$ from the axis $\boldsymbol{n}$ of easy magnetization must be small. In other words, one can put $\theta = \psi + \varepsilon$, $|\varepsilon| \ll \psi$. At the same time, because of the particle interaction with the applied field, the deviation of the vector $\boldsymbol{m}$ from the plane ($\boldsymbol{H}$, $\boldsymbol{n}$) also must be small. Therefore, the inequality $|\varphi| \ll 1$ must hold.

In the linear approximation with respect to $h_0$, $\varepsilon$ and $\varphi$, the system (3.3) reads as follows:

$$\left.\begin{aligned} &\frac{\mathrm{d}\varepsilon}{\mathrm{d}\tau} + \varepsilon\lambda\beta + \varphi\beta\sin\psi = -\lambda\sin\psi\, h_\omega,\\ &\frac{\mathrm{d}\varphi}{\mathrm{d}t}\sin\psi + \varphi\lambda\beta\sin\psi - \varepsilon\beta = \sin\psi\, h_\omega,\\ &h_\omega = h_0\cos\omega\tau. \end{aligned}\right\} \tag{3.4}$$

By using $\theta = \psi + \varepsilon$ and $m_z = \cos(\psi + \varepsilon) \approx \cos\psi - \varepsilon \sin\psi$ in the second relation (3.3), one obtains

$$w = -\frac{\omega h_0}{\Theta} \sin\psi \int_0^{\Theta} \varepsilon(\tau) \sin\omega\tau \, \mathrm{d}\tau. \tag{3.5}$$

As usual, it is convenient to present the oscillating field $h_\omega$ in the complex form $h_\omega = h_0 \exp(\mathrm{i}\omega t)$ instead of the form $h_\omega = h_0 \cos\omega t$. Solution of equation (3.7) now can be presented as follows:

$$\varepsilon = (\chi' + \mathrm{i}\chi'')h_0 \exp(\mathrm{i}\omega\tau) \sin\psi, \tag{3.6}$$

where $\chi'$ and $\chi''$ are relative real and imaginary parts of the particle dynamic susceptibility, respectively, estimated neglecting the interparticle interaction. Obviously, only the imaginary susceptibility $\chi''$ affects the dimensionless intensity $w$ of the heat production inside the particle.

The direct calculations give the following:

$$\chi'' = \lambda\omega \frac{\beta^2(1+\lambda^2) + \omega^2}{[\beta^2(1+\lambda^2) - \omega^2]^2 + 4(\beta\lambda\omega)^2}. \tag{3.7}$$

Substituting (3.7) into (3.6) and (3.5), assuming that the dimensionless time $\Theta$ of the loss energy averaging is much longer than the dimensionless period $2\pi/\omega$ of the alternating field, one obtains the following:

$$w_1 = \frac{\omega h_0^2}{2} \chi'' \sin^2\psi = \lambda \frac{\omega^2 h_0^2}{2} \sin^2\psi \frac{\beta^2(1+\lambda^2) + \omega^2}{[\beta^2(1+\lambda^2) - \omega^2]^2 + 4(\beta\lambda\omega)^2}. \tag{3.8}$$

The subscript 1 here means that the dimensionless intensity $w$ of the heat production refers to a single particle.

Let $f(\psi)$ be normalized to the unit function of distribution over the vector $\boldsymbol{n}$ orientations:

$$\int_0^{\pi} f(\psi) \sin\psi \, \mathrm{d}\psi = 1.$$

Independently of the internal morphology of particle disposition, the dimensionless intensity of the thermal effect per particle is

$$\langle w \rangle = \int_0^{\pi} w(\psi) f(\psi) \sin\psi \, \mathrm{d}\psi. \tag{3.9}$$

The average dimensional intensity of this effect per unit volume of the composite, instead of (3.3), must be calculated as follows:

$$W = \mu_0 \Phi \frac{M_\mathrm{s}^2}{t_0} \langle w \rangle. \tag{3.10}$$

Suppose that the orientation of the axis $\boldsymbol{n}$ is completely chaotic, i.e. $f(\psi) = 1/2$. In this case for the system with single particles, one obtains the following:

$$\langle w_1 \rangle = \lambda \frac{\omega^2 h_0^2}{3} \frac{\beta^2(1+\lambda^2) + \omega^2}{[\beta^2(1+\lambda^2) - \omega^2]^2 + 4(\beta\lambda\omega)^2}. \tag{3.11}$$

However, the particles can be injected into the tumour region under the action of a permanent applied field, which creates a parallel orientation of the particle axis $\boldsymbol{n}$. In this situation, the mean magnitude $\langle w \rangle$ coincides with the $w$ given in (3.9). Obviously, the maximal heat production corresponds to the perpendicular orientation of the axis $\boldsymbol{n}$ with respect to the oscillating field $\boldsymbol{H}$ ($\psi = \pi/2$). It is interesting to note that the results of [14], obtained under the assumption that the mechanism of heat production corresponds to the thermally activated Néel reorientation of the moment $\boldsymbol{m}$ through a barrier of energy $U_\mathrm{a}$, demonstrate that the thermal effect is maximal when $\psi = 0$, i.e. when the oscillating field is parallel to the particle axis of easy magnetization. We have noted that the Néel mechanism of energy dissipation must be typical for the smallest nanoparticles, whereas the discussed mechanism of remagnetization inside the potential well is for the relatively larger ones. Therefore, for particles of different sizes, from the viewpoint of heat

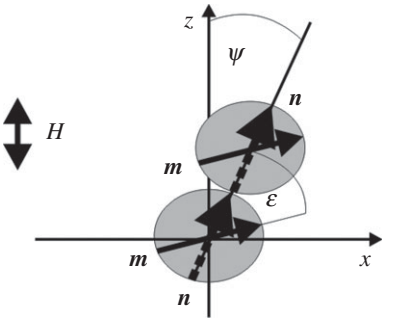


**Figure 2.** Two-particle chain.

release, different orientations of the vector $\boldsymbol{n}$ of the axis of easy magnetization, with respect to the heating field $\boldsymbol{H}$, are most efficient.

## 4. Effect of the chain-like aggregates

In this section, we will consider the two simplest chains, consisting of two and three particles. This restriction will allow us to use mathematically strict analytical approaches and to avoid any intuitive constructions. At the same time, the results will allow us to make some general conclusions on the effect of the chains as well as their size on the produced thermal effect.

### (a) Two-particle chain

Let us consider a chain cluster consisting of two particles. We will take into account that the clusters (chains) appear only because of the strong magnetic interparticle interaction; the most favourable orientation of the particle axis of easy magnetization is parallel to the axis linking the centres of the particles (the chain axis). We will assume that the particle axis of easy magnetization is aligned along the chain axis.

We introduce the Cartesian coordinate system with the axis $Oz$ directed along the oscillating field $\boldsymbol{H}$ and axis $Ox$ in the plane formed by the field $\boldsymbol{H}$ and the chain axis. This model situation is illustrated in figure 2. We neglect the thermal fluctuations of the vector $\boldsymbol{m}$, as in the previous section.

Taking into account the dipole–dipole interaction between the particles, instead of equation (3.1), now we obtain the system of equations:

$$\left.\begin{aligned} &\frac{\mathrm{d}\boldsymbol{m}_i}{\mathrm{d}\tau} = -[\boldsymbol{m}_i \times \boldsymbol{h}_i^{\mathrm{eff}}] - \lambda[\boldsymbol{m}_i \times [\boldsymbol{m}_i \times \boldsymbol{h}_i^{\mathrm{eff}}]],\\ &\boldsymbol{h}_i^{\mathrm{eff}} = \boldsymbol{h}_0 \cos\omega\tau + \beta \boldsymbol{n}_i(\boldsymbol{m}_i \cdot \boldsymbol{n}_i) + \boldsymbol{h}_i^{\mathrm{d}},\\ &\boldsymbol{h}_i^{\mathrm{d}} = \kappa \frac{3(\boldsymbol{m}_j \cdot \boldsymbol{r})\boldsymbol{r} - \boldsymbol{m}_j r^2}{r^5},\\ &i,j = 1,2, \quad i \neq j, \quad \boldsymbol{r} = \frac{\boldsymbol{R}}{d}, \quad \kappa = \frac{1}{24}. \end{aligned}\right\} \tag{4.1}$$

Here, the subscripts $i,j$ mark the particles illustrated in figure 2; $\boldsymbol{R}$ is the radius vector, linking the particles centres; $\boldsymbol{h}_i^{\mathrm{d}}$ is the dimensionless field of the dipole–dipole interaction of the $i$th particle with the $j$th one; the magnitude of the multiplier $\kappa$ directly follows from the well-known formula for the dimensional field of the dipole–dipole interaction. Under the assumption of the dense contact between the particles, the equality $r = 1$ holds.

We will again suppose that the strong inequality $h_0 \ll \beta$ is fulfilled. In this case, we can present the unit vectors of the magnetic moments directions as $\boldsymbol{m}_i = \boldsymbol{n}_i + \delta\boldsymbol{m}_i$ where $|\delta\boldsymbol{m}_i| \ll 1$, and rewrite

(3.10) in a form linear with respect to $|\delta \boldsymbol{m}_i|$. The equality $\delta \boldsymbol{m}_1 = \delta \boldsymbol{m}_2$ follows from the chain symmetry.

Taking into account the last equality, one can transform equations (3.10) to a system of two linear differential equations with respect to the angles, which describe deviations of the vectors $\boldsymbol{m}$ from $\boldsymbol{n}$ (the subscripts 1,2 of the particles number are omitted now).

Let us present the Cartesian components of vector $\boldsymbol{m}$ in the form (3.2) and put $\theta = \psi + \varepsilon$, $|\varepsilon| \ll \psi$. Here, $\psi$ again is the angle of deviation of the chain axis from the field $\boldsymbol{H}$ (see figure 2).

Because of the reasons discussed in the previous section, the angle $\varphi$ also must be small. Taking that into account, in the linear approximation with respect to $\varepsilon$ and $\varphi$, equations (4.1) can be written as follows:

$$\left.\begin{aligned}
&\frac{\mathrm{d}\varepsilon}{\mathrm{d}\tau} + \varepsilon A_\varepsilon - \varphi A_\varphi \sin\psi = \lambda h_\omega \sin\psi,\\
&\frac{\mathrm{d}\varphi}{\mathrm{d}\tau}\sin\psi + \varphi B_\varphi \sin\psi + \varepsilon B_\varepsilon = h_\omega \sin\psi,\\
&A_\varepsilon = \lambda\left[\beta + \frac{3}{24}(\sin^2\psi - \cos^2\psi)\right],\\
&A_\varphi = \beta + \frac{1}{24}(3\sin^2\psi - 1),\\
&B_\varepsilon = \beta + \frac{3}{24}(\sin^2\psi - \cos^2\psi),\\
&B_\varphi = \lambda\beta + \frac{d^3}{24r^5}[\lambda(3\sin^2\psi - 1)].
\end{aligned}\right\} \tag{4.2}$$

We again present the solution of the system (3.11) as follows:

$$\varepsilon(\psi) = (X' + \mathrm{i}X'')h_0 \exp(\mathrm{i}\omega\tau)\sin\psi, \tag{4.3}$$

where $X'$ and $X''$ are the relative real and imaginary parts of the particle dynamic susceptibility, respectively, estimated in the frames of the pair interaction between the particles. They coincide with the susceptibilities $\chi'$ and $\chi''$, defined in (3.6), of the single particle, if one formally puts $\kappa = 0$.

Note that only the imaginary part $X''$ is needed to determine the dimensionless intensity $w$ of the heat production. This part can be easily obtained from equation (14.2); however, it has a cumbersome form, which is why we omit it here.

Repeating the considerations (3.5)–(3.8), one obtains the following expressions for the dimensional intensity of the heat production by a particle in the chain:

$$w_2 = \frac{\omega h_0^2}{2} X'' \sin^2\psi. \tag{4.4}$$

The subscription 2 means here that this intensity $w$ refers to the particles in the two-particle chain. The heat production by the chain, of course, is $2w_2$.

## (b) Three-particle chain

Here, we will consider a three-particle chain. For the reasons discussed in the previous section, we will suppose that the axes of easy magnetization of all particles of the chain are parallel and the particles contact as 'head to tail'. This model situation is illustrated in figure 3.

We will number the central particle of the chains by 0, the upper and lower particles by 1 and $-1$, respectively. For the magnetic moments of each particle, we can write down the

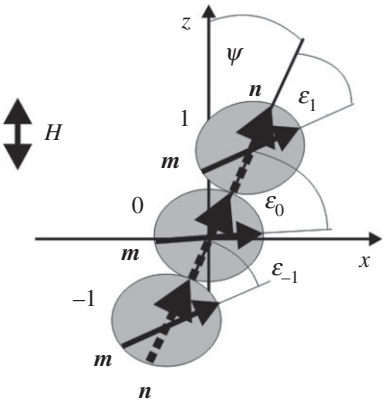


**Figure 3.** Sketch of the three-particle chain.

Landau–Lifshitz equations:

$$\left.\begin{aligned}
&\frac{\mathrm{d}\boldsymbol{m}_i}{\mathrm{d}\tau} = -[\boldsymbol{m}_i \times \boldsymbol{h}_i^{\mathrm{eff}}] - \lambda[\boldsymbol{m}_i \times [\boldsymbol{m}_i \times \boldsymbol{h}_i^{\mathrm{eff}}]],\\
&\boldsymbol{h}_i^{\mathrm{eff}} = \boldsymbol{h}_0 \cos\omega\tau + \beta \boldsymbol{n}_i(\boldsymbol{m}_i \cdot \boldsymbol{n}_i) + \boldsymbol{h}_i^{\mathrm{d}},\\
&\boldsymbol{h}_i^{\mathrm{d}} = \kappa\left[\frac{3(\boldsymbol{m}_j \cdot \boldsymbol{r}_{ij})\boldsymbol{r}_{ij} - \boldsymbol{m}_j r_{ij}^2}{r_{il}^5} + \frac{3(\boldsymbol{m}_l \cdot \boldsymbol{r}_{il})\boldsymbol{r}_{il} - \boldsymbol{m}_l r_{il}^2}{r_{il}^5}\right],\\
&i,j,l = 0,\pm 1, \quad i \neq j \neq l, \quad \boldsymbol{r}_{\mathbf{ij}} = \frac{\boldsymbol{R}_{\mathbf{ij}}}{d}, \quad \boldsymbol{r}_{\mathbf{il}} = \frac{\boldsymbol{R}_{\mathbf{il}}}{d}, \quad \kappa = \frac{1}{24}.
\end{aligned}\right\} \tag{4.5}$$

Here, $\boldsymbol{R}_{ij}$ and $\boldsymbol{R}_{il}$ are vectors linking the centre of the $i$th particle with the centres of the $j$th and $l$th ones, respectively. As earlier, we introduce the angle $\varepsilon_l$ of deviation of the unit vector $\boldsymbol{m}_l$ from the chain axis (i.e. from the axis of easy magnetization of the particles in the chain), as well as the angle $\varphi_i$ of the vector deviation from the plane $x,z$. For the reasons discussed above, we put $\varepsilon_l \ll \psi$, $|\varphi_l| \ll 1$.

Equations (4.5) can be presented in linear form with respect to the angles $\varepsilon_l$, $\varphi_l$ and the angles $\varepsilon_i$ can be written down similar to (4.3) as follows:

$$\varepsilon_l(\psi) = (X_l' + \mathrm{i}X_l'')h_0 \exp(\mathrm{i}\omega\tau)\sin\psi, \quad l = 0,\pm 1. \tag{4.6}$$

Because all considerations practically resemble those used in the derivation of equations (4.2) for the two-particle chain, we omit details. Note that the symmetry of the problem dictates the equalities $\varepsilon_{-1} = \varepsilon_1$, $\varphi_{-1} = \varphi_1$ and $X_{-1} = X_1$.

The dimensionless intensity of heat production per particle in the chain can be calculated similarly to relations (3.8) and (4.4) as follows:

$$w_3 = \frac{\omega h_0^2}{2}\frac{2X_l'' + X_0''}{3}\sin^2\psi. \tag{4.7}$$

Here, we take into account that because of symmetry $X_{-1} = X_1$.

Results of calculations of the dimensionless intensities $w_1$, $w_2$ and $w_3$ are shown in figure 4. The results demonstrate that for relatively small frequencies (the left part of figure 4), the heat production by the chains is less than that produced by the single particles; the chain is longer, the thermal effect is weaker. For relatively high frequencies (right part of figure 4), the situation is opposite—the chains enhance the effect. The peaks in the right part of figure 4 reflect the effect of the ferromagnetic resonance in the particle. This peak moves toward higher frequencies when the chain length increases.

The dimensionless frequency, corresponding to this resonance for the single particle, is $\omega_{\mathrm{r}} \approx 0.1$. By using equation (2.2), we obtain the corresponding dimensional resonance frequency

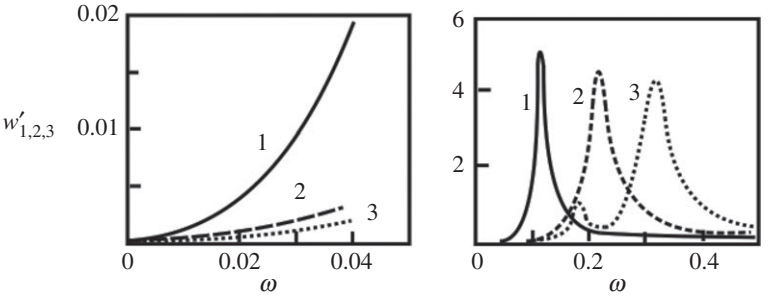


**Figure 4.** Results of calculations of the relative heat production $w'_{1,2,3} = 2/h_0^2 w_{1,2,3}$ per particle versus the dimensionless frequency $\omega$ for two intervals of the dimensionless frequency $\omega$ when $\sin\psi = 1$. Figures near curves: 1—approximation (3.8) of the single-particle chain; 2 and 3—approximations of the two-particle (equation (4.4)) and three-particle (equation (4.7)) chains, respectively.

$\Omega_r \approx 10^8\,\mathrm{s}^{-1}$. This is significantly more than the maximal frequency of the field in the hyperthermia experiments. Therefore, one can conclude that, in the range of frequencies used in the experiments, the appearance of the chains reduces the thermal effect.

## 5. Conclusion

We have studied the effect of chain-like aggregates on the magnetic hyperthermia produced by particles immobilized in a surrounding medium. We took into account that the chains can be formed by relatively large particles, whose characteristic time of Néel relaxation through the potential barrier of the particle magnetic anisotropy is much longer than the time of the hyperthermia observation. Estimates show that, for magnetite particles, this is true when the particle diameter is more than 20–25 nm. Analysis shows that, for a relatively small frequency of the applied field, the appearance of the chains weakens the thermal effect; in the range of high frequencies, it enhances it. In the range of the field frequencies used in the hyperthermia experiments, the presence of the chains reduces the thermal effect. These results must be taken into account in the interpretation of the experiments and organization of the clinical usage of magnetotherapy.

It should be noted that, in real systems, the chains must obey some law of distribution over a number of particles in the chains. The approach suggested in this paper can be used if the distribution function is known. However, the determination of this function presents a separate problem, which is beyond the scope of the paper.

Data accessibility. This article has no additional data.

Competing interests. I have no competing interests.

Funding. The work was supported by Act 211 Government of the Russian Federation, contract 02.A03.21.0006; programme of Ministry of Education and Science of the Russian Federation, 3.1438.2017/4.6; 3.5214.2017/6.7 as well as by the Russian Foundation for Basic Researches, projects 18-08-00178 and 19-52-12028.

## References

1. Shinkai M. 2002 Functional magnetic particles for medical application. *J. Biosci. Bioeng.* **94**, 606–613. (doi:10.1016/S1389-1723(02)80202-X)
2. Yu J, Huang DY, Yousaf MZ, Hou YL, Gao S. 2013 Magnetic nanoparticle-based cancer therapy. *Chin. Phys. B.* **22**, 027506. (doi:10.1088/1674-1056/22/2/027506)
3. Harabech M, Leliaert J, Coenea A, Crevecoeur G, Roost DV, Dupre L. 2017 The effect of the magnetic nanoparticle's size dependence of the relaxation time constant on the specific loss power of magnetic nanoparticle hyperthermia. *J. Magn. Magn. Mater.* **426**, 206–210. (doi:10.1016/j.jmmm.2016.11.079)

4. Egolf PW *et al.* 2016. Hyperthermia with rotating magnetic nanowires inducing heat into tumor by fluid friction. *J. Appl. Phys.* **120**, 064304. (doi:10.1063/1.4960406)
5. Dutz S, Hergt R. 2013 Magnetic nanoparticle heating and heat transfer on a microscale: basic principles, realities and physical limitations of hyperthermia for tumour therapy. *Int. J. Hypertherm.* **29**, 790–800. (doi:10.3109/02656736.2013.822993)
6. Toraya-Brown S, Fiering S. 2014 Local tumour hyperthermia as immunotherapy for metastatic cancer. *Int. J. Hypertherm.* **30**, 531–539. (doi:10.3109/02656736.2014.968640)
7. Wu K, Wang J. 2017 Magnetic hyperthermia performance of magnetite nanoparticle assemblies under different driving fields. *AIP Adv.* **7**, 056327. (doi:10.1063/1.4978458)
8. Rosensweig RE. 2002 Heating magnetic fluid with alternating magnetic field. *J. Magn. Magn. Mater.* **252**, 370. (doi:10.1016/S0304-8853(02)00706-0)
9. Odenbach S. 2002 *Magnetoviscous effect in ferrofluids*. Berlin, Germany: Springer.
10. Périgo EA, Hemrey G, Sandre O, Ortega D, Carairo E, Plazaola F, Teran FJ. 2015 Fundamentals and advances in magnetic hyperthermia. *Appl. Phys. Rev.* **2**, 041302. (doi:10.1063/1.4935688)
11. Dutz S, Kettering M, Hilger I, Müller R, Zeisberger M. 2011 Magnetic multicore nanoparticles for hyperthermia—influence of particle immobilization in tumour tissue on magnetic properties. *Nanotechnology* **22**, 265102. (doi: 10.1088/0957-4484/22/26/265102)
12. Raikher YL, Stepanov VI. 2014 Physical aspects of magnetic hyperthermia: low-frequency AC field absorption in a magnetic colloid. *J. Magn. Magn. Mater.* **368**, 421–427. (doi:10.1016/j.jmmm.2014.01.070)
13. Glockl G, Hergt R, Zeisberger M, Dutz S, Nagel S, Weitschies W. 2006 The effect of field parameters, nanoparticle properties and immobilization on the specific heating power in magnetic particle hyperthermia. *J. Phys.: Condens. Matter* **18**, S2935. (doi:10.1088/0953-8984/18/38/S27)
14. Zubarev AY, Iskakova LY, Abu-Bakr AF. 2017 Magnetic hyperthermia in solid magnetic colloids. *Physica A* **467**, 59–66. (doi:10.1016/j.physa.2016.10.045)
15. Landau LD, Lifshitz EM. 1960 *Electrodynamics of continuum media*. London, UK: Pergamon.
16. Brown Jr WF. 1963 Thermal fluctuations of a single-domain particle. *Phys. Rev.* **130**, 1677–1686. (doi:10.1103/PhysRev.130.1677)
17. Chang L *et al.* 2016 The efficiency of magnetic hyperthermia and *in vivo* histocompatibility for human-like collagen protein-coated magnetic nanoparticles. *Int. J. Nanomed.* **11**, 1175–1185. (doi:10.2147/IJN.S101741)
18. Trahms L. 2009 In *Colloidal magnetic fluids. Basics, development and application of ferrofluids* (ed. S Odenbach). Berlin, Germany: Springer.
19. Carrey J, Mehdaoui B, Respaud M. 2011 Simple models for dynamic hysteresis loop calculations of magnetic single-domain nanoparticles: application to magnetic hyperthermia optimization. *J. Appl. Phys.* **109**, 033901. (doi:10.1063/1.3551582)
20. Mehdaoui B, Tan RP, Meffre A, Carrey J, Lachaize S, Chaudret B, Respaud M. 2013 Increase of magnetic hyperthermia efficiency due to dipolar interactions in low-anisotropy magnetic nanoparticles: theoretical and experimental results. *Phys. Rev. B* **87**, 174419. (doi:10.1103/PhysRevB.87.174419)
21. Dennis CL, Jackson AJ, Borchers JA, Hoopes PJ, Ivkov R, Foreman AR, Lau JW, Goernitz E, Gruettner G. 2008 The influence of collective behavior on the magnetic and heating properties of iron oxide nanoparticles. *J. Appl. Phys.* **103**, 07A319. (doi:10.1063/1.2837647)
22. Gudoshnikov SA, Liubimov BY, Usov NA. 2012 Hysteresis losses in a dense superparamagnetic nanoparticle assembly. *AIP Adv.* **2**, 012143. (doi:10.1063/1.3688084)
23. Urtizberea A, Natividad E, Arizaga A, Castro M, Mediano A. 2010. Specific absorption rates and magnetic properties of ferrofluids with interaction effects at low concentrations. *J. Phys. Chem. C* **114**, 4916–4922. (doi:10.1021/jp912076f)
24. Martinez-Boubeta C *et al.* 2012 Adjustable hyperthermia response of self-assembled ferromagnetic Fe–MgO core–shell nanoparticles by tuning dipole–dipole interactions. *Adv. Funct. Mater.* **22**, 3737. (doi:10.1002/adfm.201200307)
25. Landau LD, Lifshitz EM. 1965 In *Collected papers of L. D. Landau* (ed. D. Ter Haar), p. 101. London, UK: Pergamon.
26. Aharoni A. 1996 *Introduction to the theory of ferromagnetism*. Oxford, UK: Clarendon.
27. Brown WF. 1978 *Micromagnetics*. Huntington, NY: Robert E. Krieger.